Gain and lifetime of GaInNAsSb narrow ridge waveguide laser diodes in continuous-wave operation at 1.56 mm

Gupta, J. A.; Barrios, P. J.; Caballero, J. A.; Poitras, D.; Aers, G. C.; Pakulski, G.; Wu, X.

Publisher's version / Version de l'éditeur:
https://doi.org/10.1063/1.2361179
Applied physics letters, 89, 2006

Gain and lifetime of GaInNAsSb narrow ridge waveguide laser diodes in continuous-wave operation at 1.56 μm

J. A. Gupta,[a] P. J. Barrios, J. A. Caballero, D. Poitras, G. C. Aers, G. Pakulski, and X. Wu
Institute for Microstructural Sciences, National Research Council of Canada, Ottawa, Ontario K1A 0R6, Canada

(Received 6 July 2006; accepted 25 August 2006; published online 11 October 2006)

The continuous-wave (cw) operation of GaInNAsSb lasers at 1560 nm is reported. Light-current measurements were made before and after a 100 h cw burn in at 20 °C, during which a 3×890 μm^2 device with 72 mA initial threshold current and 14 mW maximum output power experienced a 15% drop in peak output power. These preliminary lifetime results provide insight into the reliability of GaInNAsSb active regions and reinforce the promise of this material for C-band devices. High-resolution modal gain spectra were extracted from the amplified spontaneous emission spectra acquired after the burn in, providing reliable values for the internal loss, transparency current, and differential gain. © *2006 American Institute of Physics*.
[DOI: 10.1063/1.2361179]

The addition of Sb to GaInNAs has greatly accelerated 1.55 μm laser development on GaAs.[1] Although promising results have been obtained for Sb-free 1.5 μm lasers grown by metal organic vapor phase epitaxy[2] and molecular beam epitaxy (MBE),[3,4] more rapid progress towards longer wavelength cw operation has been made with the quinary material[5–8] which benefits from the Sb surfactant effect.[1,9]

In this letter we report GaInNAsSb/GaNAs double quantum well (QW) ridge waveguide (RWG) lasers with a room-temperature cw lasing wavelength of 1.56 μm. The devices were burned in for 100 h to evaluate their reliability and to ensure stability for subsequent measurements. The temperature performance was studied between 5 and 45 °C in cw mode. Modal gain was studied in a single-lateral mode RWG device using the amplified spontaneous emission (ASE) spectra below threshold. This provided reliable values for the internal loss, transparency current, and differential gain.

MBE growth of the GaInNAsSb QWs was described in detail recently.[9] The laser structure was grown on a N^+GaAs substrate and contains Si (2×10^{18} cm^{-3}) and Be-doped (1×10^{18} cm^{-3}) $Al_{0.33}Ga_{0.67}As$ cladding layers grown at 610 °C. To reduce lateral leakage current and free-carrier absorption,[10] the Si and Be concentrations were reduced to 5×10^{17} and 3×10^{17} cm^{-3} in the 200 and 250 nm cladding regions closest to the waveguide, respectively. Undoped digital-alloy grading was used between the cladding layers and the GaAs waveguide. The active region, grown at 420 °C, nominally consists of two 7 nm $Ga_{0.6}In_{0.4}N_{0.027}As_{0.9605}Sb_{0.0125}$ QWs with 7.5 nm $GaN_{0.045}As_{0.955}$ barriers. A 5 nm intermediate GaAs layer provided a total QW separation of 20 nm. The active region was embedded in a $1-\lambda$ GaAs waveguide for $\lambda = 1.55$ μm. Doped digital-alloy grading was used between the cladding layers and the 100 nm GaAs:Be (1×10^{19} cm^{-3}) and 200 nm GaAs:Si (2×10^{18} cm^{-3}) contact layers. No additional *ex situ* annealing was performed before device fabrication.

RWG lasers were fabricated using inductively coupled-plasma reactive ion etching with TiPtAu and NiGeAu *p*- and *n*-contact metallizations. The lasers were cleaved into Fabry-Pérot cavities and the back facets were coated with *a*-Si/SiO_2 high-reflectivity (HR) (92%) coatings using plasma-enhanced chemical vapor deposition. The coated devices were mounted *p* side up onto alumina carriers and tested on a Cu thermoelectric stage. The cw output power was measured using a calibrated InGaAs detector, and the emission spectra were measured using a tapered fiber coupled to an Ando AQ6317 optical spectrum analyzer.

Figure 1 shows the temperature-dependent cw measurements of a 3×890 μm^2 device before burn in. The initial threshold current was 59 mA (72 mA) with a maximum output power of 20 mW (14 mW) at 5 °C (20 °C). Just above threshold, the device exhibits cw light output near 1560 nm at 20 °C (Fig. 2). The emission blueshifts with decreasing temperature to 1549 nm at 5 °C. The cw characteristic temperature T_0 was found to be 71 K from 5 to 30 °C, similar to the value reported in Ref. 8. The cw operating temperature of 45 °C is the highest yet reported for GaAs-based laser diodes near 1550 nm. The present devices suffer from higher

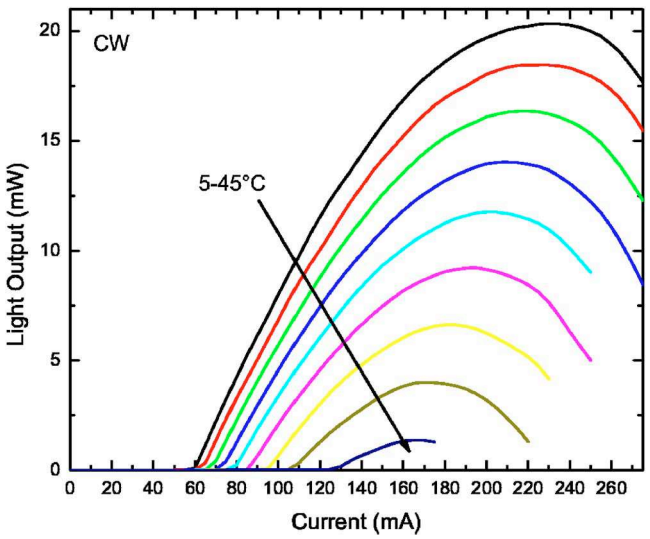

FIG. 1. (Color online) Temperature-dependent cw light output (L) vs current (I) for a 3×890 μm^2 laser before burn in.

[a]Electronic mail: james.gupta@nrc.ca

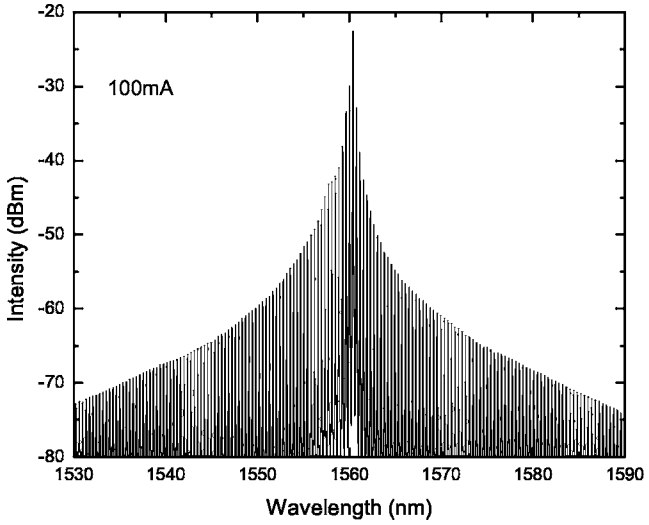

FIG. 2. cw output spectrum with 100 mA drive current at 20 °C acquired after the burn in.

threshold voltage (~2 V) and differential resistance compared with our previous report,[6] likely due to insufficient doping in the cladding regions closest to the waveguide. This reinforces the importance of balancing the laser design to reduce lateral leakage current and free-carrier absorption while minimizing the series resistance.

To assess the device reliability, the same laser was driven in cw mode at 140 mA and 20 °C for 100 h. As shown in Fig. 3, the output power decreased by about 25% from the initial value over this time. After the burn in, the threshold current increased to 84 mA, while the maximum output power decreased to 12 mW. Other lasers from the same batch exhibited similar characteristics over the same test period with no device failures. Thus the 100 h cw operation should be viewed as a lower limit for the lifetime.

The optical gain was extracted using Cassidy's method[11] which uses the ratio of the average mode intensity to the valley intensity. This method is less sensitive to the wavelength resolution of the measurement system and enables above-threshold gain measurements. The ASE spectra were

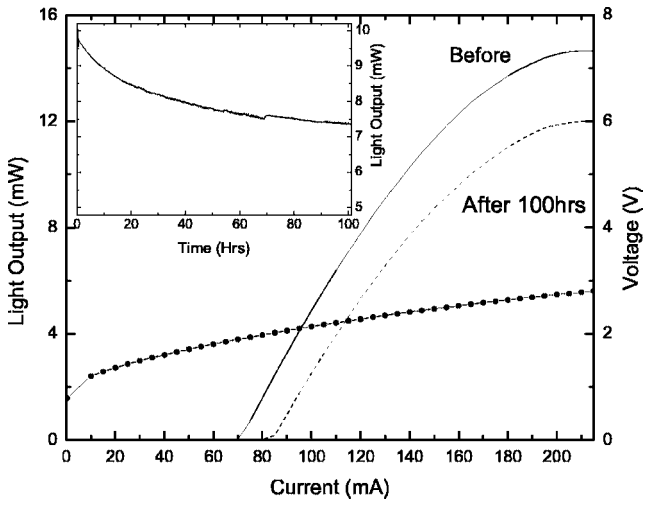

FIG. 3. Comparison between cw light output and current at 20 °C for the same device before (solid) and after (dashed line) burn in. The inset shows the output power during cw burn in at 20 °C at constant current of 140 mA. The solid line with circles indicates the current-voltage dependence.

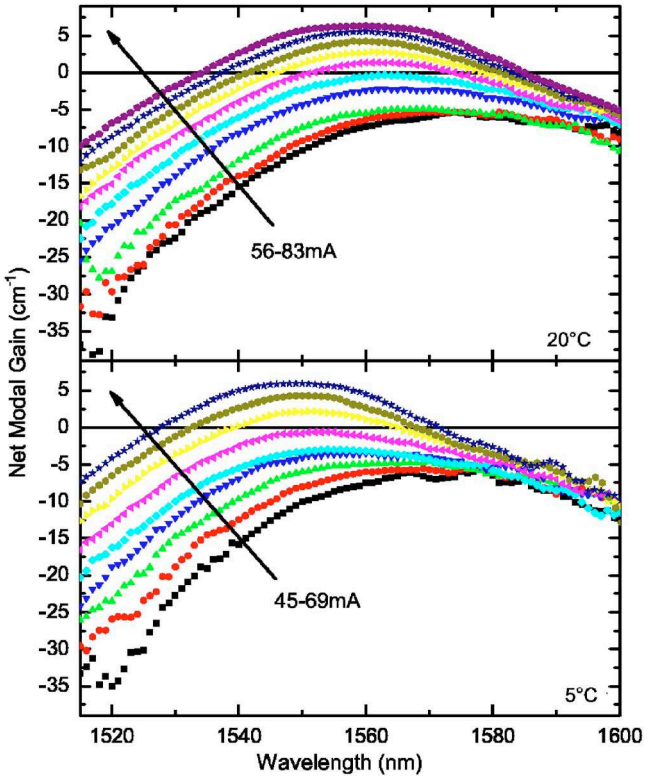

FIG. 4. (Color online) cw net modal gain spectra at 5 °C (bottom) and 20 °C (top). The ASE spectra were acquired at 3 mA intervals.

acquired at 5 and 20 °C at a resolution of 0.1 nm, yielding the gain spectra of Fig. 4. The modal gain $G=\Gamma g$ depends on the material gain g, and for this laser structure the confinement was calculated to be $\Gamma=0.0266$ using an effective index mode solver. The net modal gain is $G_{\text{net}}=\Gamma g-\alpha_i$, and at long wavelength the gain spectra converge to the internal loss α_i with approximate values near 8 ± 2 and 9 ± 2 cm^{-1} at 5 and 20 °C, respectively. At threshold the net modal gain clamps at the mirror loss, which is calculated for this device to be 6.75 cm^{-1}, where $\alpha_m=[1/(2L)]\ln(1/R_1R_2)$, L is the cavity length, and $R_1=0.92$ and $R_2=0.33$ are the HR and as-cleaved mirror reflectivities, respectively. Measurements of the available gain in these QW materials would benefit from shorter, uncoated devices having higher mirror losses, for which the gain is clamped at higher values. Figure 5 shows the variation in the peak material gain with increasing injection current. With no clamping at the mirror loss, the peak gain would follow a logarithmic dependence on the carrier density.[12,13] Using the measured values of internal loss, the material gain at threshold is near 570 cm^{-1} at both temperatures. With increasing current injection, the gain is blueshifted to shorter wavelengths (Fig. 5), although the emission peak is actually redshifted because of active region heating due to the large series resistance.

The transparency currents were found to be 62 and 69 mA at 5 and 20 °C, respectively. Since these values include the lateral leakage current, the true transparency current densities are slightly lower than these values suggest. For this narrow RWG, the threshold current also includes a diffusion component, since the ridge width is similar to the carrier diffusion length inside the QWs.[5,14] The differential gain dG/dI at transparency is 0.836 cm^{-1}/mA at 5 °C and 0.635 cm^{-1}/mA at 20 °C. These values are lower than for 1.3 μm GaInNAs lasers,[15] while it was noted in Ref. 16 that

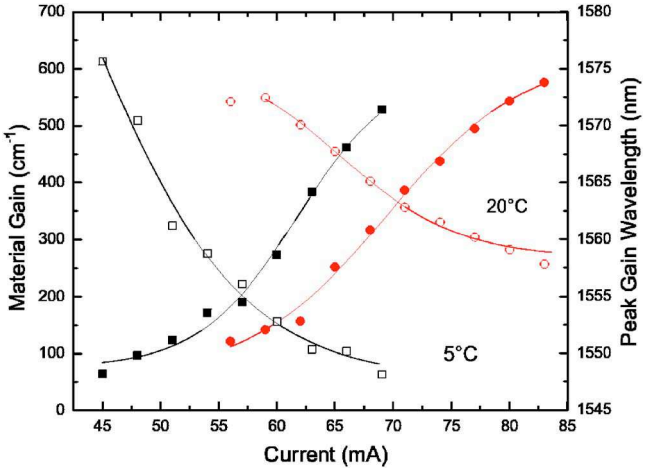

FIG. 5. (Color online) Dependence of peak material gain (filled symbols) and peak gain wavelength (open symbols) on injection current at 5 °C (squares) and 20 °C (circles). The solid lines are guides for the eyes, based on the best fits assuming a sigmoidal dependence.

the differential gain in GaInNAs is lower than in pure GaInAs with the introduction of even 0.25% nitrogen due to the strong coupling between the N resonant band and the conduction band edge states.

In summary, GaInNAsSb narrow RWG laser diodes were tested before and after 100 h of room-temperature cw operation. The devices showed limited degradation during the burn in but reached a stable performance level, allowing modal gain spectral measurements. While the internal losses have been significantly reduced compared to our previous work,[6] the characteristics are still limited by high series resistance. Future work will strike a balance between low resistance and minimized lateral leakage and absorption losses associated with heavily doped cladding layers. This should allow the demonstration of low-threshold devices with higher output power and improved temperature stability.

The authors are grateful for the technical support of P. Chow-Chong, G. I. Sproule, R. Wang, S. Moisa, and M. Bresee and helpful discussions with Z. R. Wasilewski.

[1]X. Yang, M. J. Jurkovic, J. B. Heroux, and W. I. Wang, Appl. Phys. Lett. **75**, 178 (1999).
[2]M. Yokozeki, J. Mitomo, Y. Sato, T. Hino, and H. Narui, Electron. Lett. **40**, 1060 (2004).
[3]M. Hugues, B. Damilano, J. Barjon, J.-Y. Duboz, J. Massies, J.-M. Ulloa, M. Montes, and A. Hierro, Electron. Lett. **41**, 595 (2005).
[4]G. Jaschke, R. Averbeck, L. Geelhaar, and H. Riechert, J. Cryst. Growth **278**, 224 (2005).
[5]J. A. Gupta, P. J. Barrios, X. Zhang, G. Pakulski, and X. Wu, Electron. Lett. **41**, 71 (2005).
[6]J. A. Gupta, P. J. Barrios, X. Zhang, J. Laponte, G. Pakulski, X. Wu, and A. Delâge, Electron. Lett. **41**, 1060 (2005).
[7]Z. C. Niu, S. Y. Zhang, H. Q. Ni, D. H. Wu, H. Zhao, H. L. Peng, Y. Q. Xu, S. Y. Li, Z. H. He, Z. W. Ren, Q. Han, X. H. Yang, Y. Du, and R. H. Wu, Appl. Phys. Lett. **87**, 231121 (2005).
[8]S. R. Bank, H. P. Bae, H. B. Yuen, M. A. Wistey, L. L. Goddard, and J. S. Harris, Electron. Lett. **42**, 156 (2006).
[9]J. A. Gupta, G. I. Sproule, X. Wu, and Z. R. Wasilewski, J. Cryst. Growth **291**, 86 (2006).
[10]S. R. Bank, M. A. Wistey, L. L. Goddard, H. B. Yuen, V. Lordi, and J. S. Harris, Jr., IEEE J. Quantum Electron. **40**, 656 (2004).
[11]D. T. Cassidy, J. Appl. Phys. **56**, 3096 (1984).
[12]L. L. Goddard, S. R. Bank, M. A. Wistey, H. B. Yuen, Z. Rao, and J. S. Harris, Jr., J. Appl. Phys. **97**, 083101 (2005).
[13]L. A. Coldren and S. W. Corzine, *Diode Lasers and Photonic Integrated Circuits* (Wiley, New York, 1995).
[14]S. Y. Hu, D. B. Young, A. C. Gossard, and L. A. Coldren, IEEE J. Quantum Electron. **30**, 2245 (1994).
[15]X. Zhang, J. A. Gupta, P. J. Barrios, G. Pakulski, X. Wu, and A. Delâge, J. Vac. Sci. Technol. A **24**, 787 (2006).
[16]S. Tomic, E. P. O'Reilly, R. Fehse, S. J. Sweeney, A. R. Adams, A. D. Andreev, S. A. Choulis, T. J. C. Hosea, and H. Reichert, IEEE J. Sel. Top. Quantum Electron. **9**, 1228 (2003).